The final publication is available at

https://doi.org/10.1109/TIE.2008.2004378

Additional Information

A general approach for the transient detection of slip-dependant fault components based on the Discrete Wavelet Transform

M. Riera-Guasp, J.A. Antonino Daviu, M. Pineda-Sánchez, R. Puche-Panadero, J. Pérez-Cruz

Abstract— **In this paper, a general methodology based on the application of the Discrete Wavelet Transform (DWT) to the diagnosis of cage motors condition using the transient stator currents is exposed. The approach is based on the identification of characteristics patterns introduced by fault components in the wavelets signals obtained from the DWT of transient stator currents. These signals enable a reliable detection of the corresponding fault, as well as a clear interpretation of the physical phenomenon taking place in the machine. A compilation of the application of the methodology to several fault cases such as the presence of rotor asymmetries or eccentricities, is done. Guidelines for the easy application of the methodology by any user are also provided under a didactic perspective.**

Index Terms--**Induction motors, wavelet transforms, fault diagnosis, transient analysis.**

I. INTRODUCTION

IN the industrial environment, the stator current is often used for the diagnosis of a wide range of electromechanical faults in cage induction motors. This is a quantity easy to be measured in a simple and non-invasive way. Indeed, the study of the Fourier spectrum of the steady-state current has hitherto revealed as the most reliable way for the diagnosis of many different faults [1], such as rotor asymmetries [2-3], eccentricities (static, dynamic or mixed) [4], or even inter-turn short-circuits [5-6]. These faults introduce particular frequencies in the spectrum, which are used for the diagnosis of the corresponding failure.

Nevertheless, in the industrial environment, the Fourier spectrum is usually polluted with other frequencies caused by the slotting, non-ideal winding distribution, perturbations in the operation of the machine, noises, transient oscillations or even rotor imperfections due to the manufacturing process [7-9]. All these facts may make the diagnosis certainly difficult, mainly taking into account that these phenomena are very usual in the real industrial life.

For instance, the presence of load oscillations, quite common when the machine drives mills, compressors, pumps or other mechanisms involving gear reducers, introduces frequencies in the Fourier spectrum which might be very similar to those used for the diagnosis of rotor asymmetries or even eccentricities [7-9]. This can lead to confusion or even to a wrong diagnosis of these faults.

Moreover, the application scope for the steady-state based approaches is sometimes restricted. For instance, the detection of broken rotor bars through the sideband components appearing in the Fourier spectrum is only valid if the machine operates under a certain level of load [7-8]. This fact implies the necessity of loading the machine before carrying out the steady-state current measurements for condition monitoring purposes.

Other drawbacks such as the influence of interbar currents on the amplitude of the components used for the diagnosis of rotor asymmetries [10] or the difficulties when diagnosing the condition of the outer cage in double cage rotors [11] has been also reported by other authors as additional drawbacks of the steady-state based methods.

These and other reasons have led some authors during these recent years to propose the study of the transient processes of the machine as a way to obtain additional information which could complement that provided by the traditional steady-state-based methods. In this context, the study of the startup transient has drawn most of the attention. A great amount of works have been focused on the detection of a particular fault: the presence of rotor asymmetries in the machine.

Some contributions during the 80's and early 90's [12-13] already proposed the study of the startup transient for diagnosis purposes. However, the signal processing techniques available at that time were not suitable for the analysis of transient signals such as the startup current. During the 90's an important research was carried out by a group of English authors for the diagnosis of broken bars; the basis of these contributions was to detect the presence of the left sideband harmonic, created by the rotor asymmetry, during the startup transient. For this purpose, filtering techniques were proposed firstly [11, 14], although a certain complexity on the methodology and high computational requirements were needed. These authors even introduced the possibility of applying the wavelet theory for the detection of this component, through the convolution of the startup current signal with a Gaussian wavelet [15-17]. Nevertheless, the development of the wavelet theory was not enough advanced, so the three-dimensional patterns resulting from the analyses did not seem clear enough. In addition, the detection of the sideband harmonic evolution was circumscribed to a narrow frequency band.

Despite this fact, these works represented a clear advance, not only because they introduced the idea of fault components evolving during the transient, but also because they even provide some quantitative values based on the results of transient analysis, which were expected to serve as a reference for quantifying the degree of failure. In addition, they were one of the pioneers in proposing the possibility of application of

Authors are with Universidad Politecnica de Valencia, Dept. of Electrical Engineering, Institute of Energy Engineering, Camino de Vera s/n, 46022, Valencia, SPAIN (e-mails: mriera@die.upv.es; joanda@die.upv.es; mpineda@die.upv.es; rupucpa@die.upv.es; juperez@die.upv.es).

the wavelet theory to the transient analysis for diagnosis purposes, although they did not deep in this field.

During this last decade, in parallel with the advances in the wavelet theory and the optimization of its different modalities (Continuous Wavelet Transform (CWT), Discrete Wavelet Transform (DWT), Wavelet Packets…), new wavelet-based diagnosis methods focused on the analysis of the startup current have been proposed; in [18] the wavelet coefficients were used for the detection of broken bars. The 'wavelet ridge' was proposed in [19] for the diagnosis of the same fault. [20] proposed the application of the DWT for the prognosis of other electromechanical faults. Other more recent examples regarding the application of wavelets to the diagnosis can be found in [21-24].

Moreover, other techniques based on the use of digital filters have been proposed [25-26]. They can be considered as equivalent alternatives for extracting the time evolution of fault components, showing clear similarities with the filtering process carried out by the DWT.

In addition, other modern time frequency decomposition tools, currently under development, such as the Hilbert-Huang Transform, have been recently proposed for the diagnosis of different electromechanical faults such as bearing faults or rotor asymmetries [27-30].

The implicit or explicit basis of the aforementioned contributions is the detection of the presence during the transient of characteristic components caused by the corresponding fault, most of the times by means of an indirect indicator (increments in wavelets coefficients, wavelet ridge…).

In this context, the authors of this paper proposed a method based on the application of the Discrete Wavelet Transform (DWT) to the startup current. This tool enables not only the mere indirect detection but also the extraction of the transient evolution of components caused by rotor asymmetries [8-9, 26-27, 31-32]. The method was based on the study of the wavelet signals (approximation and details) resulting from the DWT. The band-pass filtering performed by these signals enables the transient extraction of the harmonic components caused by the corresponding faults, arising characteristic patterns associated with each failure. These patterns make possible a reliable diagnosis of the faults since the particular transient evolution of each component is very unlikely to be caused by other phenomena different from that fault. Moreover, the patterns enable the discrimination between faults through the different waveforms appearing in the wavelet signals.

One important advantage of the methodology is the clear relation which can be established between the oscillations appearing in the wavelet signals resulting from the analysis and the physical phenomenon taking place in the machine, a fact not always possible with some of the aforementioned transient-based approaches.

The validity of the proposed method was assessed for the diagnosis of rotor asymmetries in a wide range of machines and sizes, from real and laboratory motors with small sizes [8, 31-32] to large motors on the order of MW, operating in real power generation plants [26]. Moreover, its validity for the diagnosis of other faults such as dynamic eccentricities has been also proven [9].

Furthermore, the qualitative nature of the proposed methodology was complemented through the introduction of non-dimensional parameters, based on the energy of the wavelet signals. These parameters enable the quantification of the degree of failure, for the case of rotor asymmetries.

The proposed DWT-based methodology, together with the transient approaches before commented, can be considered as representative of a new trend, the *Transient Motor Current Signature Analysis* (TMCSA), developed in order to complement and, in some cases, overcome the deficiencies of the traditional MCSA approach.

This work is intended to be a didactic explanation of the DWT diagnosis methodology developed by the authors, so that every user reading it could easily follow the guidelines for its real application in the industrial environment. A compilation of real diagnosis cases regarding different faults (rotor asymmetries, eccentricities) serves as an illustrative basis to support the explanation.

The paper is organized as follows; in Section II, the physical bases of the methodology are introduced. Section III introduces the main concepts about the DWT regarding its utilization for analyzing transient current signals. Section IV provides the guidelines for the application of the method, under a didactic perspective. A compilation of real diagnosis cases is presented in Section V, including rotor asymmetries and mixed eccentricities. Section VI summarizes the non-dimensional parameters defined for the quantification of the degree of failure. Finally, the conclusions of the work are presented.

II. PHYSICAL BASES OF THE METHOD

A. Rotor asymmetries.

As it is well-known, when a rotor bar breaks, the current cannot circulate trough it. Subsequently, a perturbation (fault field) superimposes to the normal air-gap field. In steady-state, the fault field induces some current components in the stator windings, with characteristic frequencies. The amplitudes of these components depend on the constructive parameters of the machine, on the load condition and on the inertia of the motor-load group. Their frequencies can be calculated according to (1) and (2) [1-3].

$$f_b = \left(1 \pm 2 \cdot k \cdot s\right) \cdot f \qquad k = 1,2,3.... \qquad (1)$$

$$f_b = \left(\frac{k}{p}(1-s) \pm s\right) \cdot f \qquad \frac{k}{p} = 1,3,5.... \qquad (2)$$

where f_b: detectable bar breakage frequencies; p: number of pole pairs; f: supply frequency; s: slip.

Among these components, those normally used in the industrial environment for the diagnosis of rotor asymmetries are the main *sideband components* appearing around the supply frequency and given by (3) (left sideband (negative sign) and right sideband (positive sign)).

$$f_b = \left(1 \pm 2 \cdot s\right) \cdot f \qquad (3)$$

The use of other high order harmonics in expressions (1) and (2) can imply also some benefits, since their amplitudes are less likely to be affected by load torque oscillations or even

by interbar currents [10, 33]. However, their amplitudes are usually much lower than those of the sidebands and, in some cases, due to their dependence on the winding factor of the machine, they may have so low amplitudes that their measurement becomes almost impossible [33]. This is the reason why the diagnosis has been mainly focused on the study of the main sidebands around the supply frequency and, more concretely, on the left sideband, since often it has a higher amplitude than that of the right sideband [34].

During the startup transient, as the speed increases, the slip s changes from 1, when the machine connects, to almost zero (when the steady-state regime is reached). This change in the slip leads to a variation of the slip-dependant fault components and, among them, of the left sideband component [14]. In previous works [32], combining the Deleroi's approach for studying the bar breakage phenomenon [35] with the space vectors theory [36], the theoretical evolution of the left sideband component during the startup was justified, not only in frequency but also in amplitude. Fig. 1 shows the theoretical waveform of the left sideband component flowing through one stator phase during the startup transient for a faulty machine. This waveform was deduced in [32], using a numerical model of a 1.1 kW induction motor with 2 pole pairs and 1 broken bar.
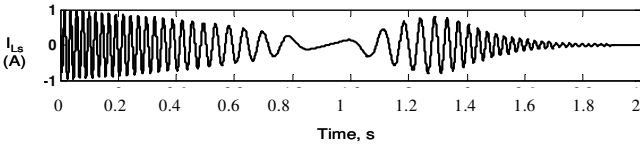

Fig. 1. Waveform of the left sideband component during the startup transient for a 1.1 kW , 4-pole motor with 1 broken bar.

The frequency and amplitude of the left sideband evolve in a characteristic way during the startup: The frequency, at the beginning, is equal to the supply frequency f. As the slip s decreases during the startup, the frequency of the sideband decreases firstly until becoming zero. Then, it increases again until reaching a value near the supply frequency f. This evolution is in agreement with the expression for the frequency of the left sideband in steady-state, given by (3). Regarding the sideband amplitude, it decreases firstly from an initial value, until the slip equals 0.5. Then, it increases until reaching a maximum value (higher than the initial amplitude) and it decreases again until reaching the steady-state amplitude. The description and analysis of this evolution is also done in [32].

Another transient wich involves substantial changes in the value of slip s and so in the sideband frequencies is the plug stopping; it is used in industrial drives when a quick stop of the machine is needed. Braking is achieved by reversal of the stator connections while the motor is running, so reversing the direction of the traveling-wave airgap field [37].

During this transient, the slip s changes from almost 2 (field rotating in the inverse direction at the synchronous speed) to 1 (motor stopped). Therefore, a characteristic evolution in the left sideband will arise. Fig.2 shows the simulated evolution of the sideband during this braking mode, using the numerical model commented before for the machine with one broken bar.

As it can be observed there, the frequency of the sideband during this transient evolves from ~150 Hz ($s \approx 2$) to 50 Hz (s=1), in agreement with the expression (3), valid for steady-

state. Thus the tracing of the sideband, during the braking mode can also constitute a reliable indicator of the presence of the asymmetry.
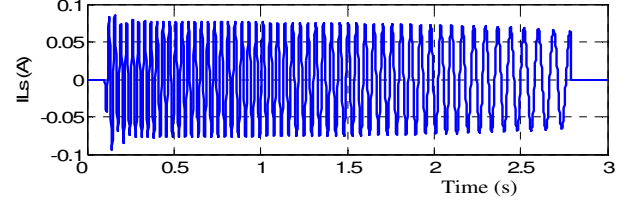

Fig. 2. Waveform of the left sideband component during plug braking for a 1.1 kW , 4-pole motor with 1 broken bar.

B. Mixed eccentricities.

In an asynchronous machine, the eccentricity is reflected through a non-uniform air-gap between stator and rotor. There are two main types of eccentricity; the static eccentricity and the dynamic eccentricity. In the case of the static eccentricity the position of minimum air-gap remains fixed in space. This can be caused by several reasons such as ovality of the stator, or an incorrect placement of the rotor or stator during the assembly process [38]. The dynamic eccentricity appears when the rotation axis of the rotor does not coincide with its geometric axis. This fact causes that the position of minimum air-gap changes with time. This eccentricity can be due to reasons such as deformation of the rotor shaft, bearing wear or misalignment or mechanical resonance at critical speed [38]. Often both these types of eccentricity coexist, being unusual to find a pure dynamic or static eccentricity.

Several authors have given expressions for the calculation of the frequencies introduced by static or dynamic eccentricities. If both types of eccentricities coexist (mixed eccentricities), low frequency components near the fundamental appear [39]. These frequency components are given by (4), where f_r is the rotational frequency.

$$f_{ecc} = f \pm k \cdot f_r \quad , \quad k=1,2,3\ldots \quad (4)$$

Equivalent expressions, such as (5), have also been provided by other authors [1].

$$f_{ecc} = f \left[1 \pm m \frac{1-s}{p} \right] \quad , \quad m=1,2,3\ldots \quad (5)$$

As observed, (5) depends on the slip s. If $m=p/2$, during the startup transient, as the slip s varies from 1 to 0, two components associated with the eccentricity will evolve in a very characteristic way; the frequency of the first one will start being equal to the supply frequency f (s=1) and will decrease, reaching $f/2$ when the steady-state is reached ($s \approx 0$). The second component will start being equal to f (s=1) evolving towards $3 \cdot f/2$ ($s \approx 0$). The tracing of these two components during the startup have been also proven to be a reliable way for the detection of eccentricities [9].

III. BASES OF THE DIAGNOSIS APPROACH

A. The Discrete Wavelet Transform (DWT)

The main idea that underlies the application of the DWT is the dyadic band pass filtering process carried out by this transform. Provided a certain sampled signal s= (i_1, i_2, $\ldots i_N$) ,

the DWT decomposes it onto several wavelet signals (an approximation signal a_n and n detail signals d_j) [8, 40]. A certain frequency band is associated with each wavelet signal; the wavelet signal reflects the time evolution of the frequency components of the original signal s which are contained within its associated frequency band [8, 41].

More concretely, if f_s (samples/s) is the sampling rate used for capturing s, then the detail d_j contains the information concerning the signal components with frequencies included in the interval:

$$f(d_j)\in[2^{-(j+1)}f_s,\ 2^{-j}f_s]\ Hz. \qquad (6)$$

The approximation signal a_n includes the low frequency components of the signal, belonging to the interval:

$$f(a_n)\in[\ 0,\ 2^{-(n+1)}f_s]\ Hz \qquad (7)$$

Therefore, the DWT carries out the filtering process shown in Fig. 3. Note that the filtering is not ideal, a fact leading to a certain overlap between adjacent frequency bands [8, 31, 42]. This causes some distortion if a certain frequency component of the signal is close to the limit of a band.
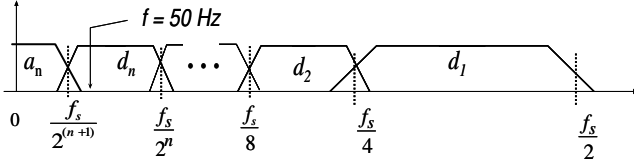

Fig. 3. Filtering process performed by the DWT.

Due to the automatic filtering performed by the wavelet transform, the tool provides a very attractive flexibility for the simultaneous analysis of the transient evolution of rather different frequency components present in the same signal. At the same time, in comparison with other tools, the computational requirements are low. In addition, the DWT is available in standard commercial software packages, so no special or complex algorithm is required for its application.

B. Some wavelet patterns of common fault related time-frequency varying components

In this section the DWT is applied to analytically generated signals. Some of these signals reproduce the related fault components that were previously described. The aim of this section is twofold; first, the practical application of DWT to known signals will help to understand how this mathematical tool operates. The second objective is to make easier the task of recognizing these fault related patterns when analyzing an experimental signal.

1. Multi-cosine signal

This example illustrates how the DWT performs an automatic filtering process, extracting components of different frequencies from a complex signal. Fig. 4 shows the DWT of a signal s generated as the superposition of two cosines with equal amplitude but different frequencies (12 Hz and 50 Hz); the signal was sampled at 1 kHz. The DWT extracts both pure-tone components, placing them into the wavelets signals d4 and d6, the associated frequency bands of which -calculated

according (6)- include the frequencies of 50 and 12 Hz respectively.

In Fig. 5 the signal s is generated by concatenating both cosines. This example illustrates how the DWT enables the time-frequency analysis, showing not only the components of the signal, but also the time in which these components exist.

On the other hand, traditional Fourier transform performs an analysis in the frequency-only domain; Fig.6 shows the Fourier spectra of signals s in Figs. 4 and 5. Both spectra are identical,
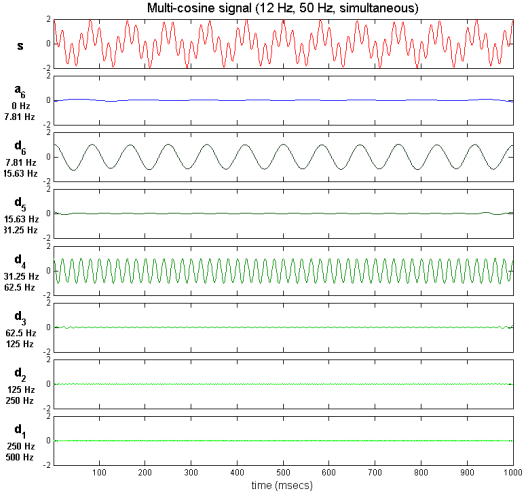

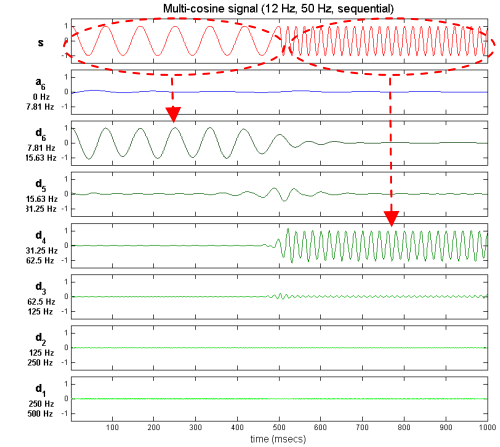Fig.4. Wavelet decomposition of a multi-cosine signal based on two simultaneous cosines of 12 Hz and 50 Hz.

Fig. 5 Wavelet decomposition of a multi-cosine signal based on the concatenation of two consecutive cosines of 12 Hz and 50 Hz.
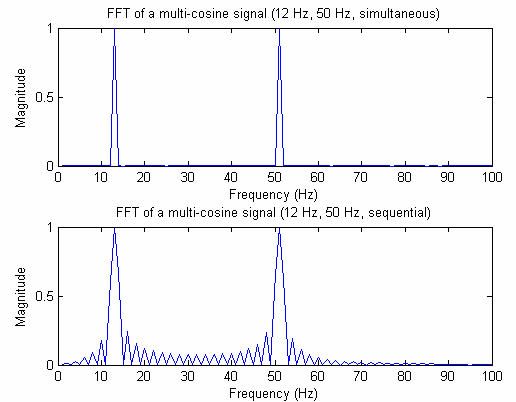

Fig.6. FFT of a multi-cosine signal (12 Hz, 50 Hz) simultaneous (top) and consecutive (bottom).

because Fourier transform provides the frequencies of the components included into the signal but it is not able to inform about the time in which these components occur.

2. *Linear swept -frequency cosine signal*

A linear swept-frequency cosine has been generated during 4 seconds, varying from 0 Hz to 75 Hz during the first half of the sampling time, and from 75 Hz down to 0 Hz during the second half. The frequency of this signal evolves with time in a similar way to that of the left sideband for a machine with rotor asymmetry during the startup. It has been sampled at 1 kHz, and the resulting wavelet decomposition is shown in Fig. 7. The portion of signal s with decreasing frequency (0<t<2000 ms) is reflected in the decomposition as a succession of oscillations moving from low order (high frequency) details towards high order (low frequency) ones. This pattern appears thanks to the filtering performed by DWT: Each wavelet signal reproduces the portion of signal *s* the frequencies of which are included within the wavelet signal.

Accordingly, the portion of signal s with increasing frequency (2000<t<4000ms) is reflected in the decomposition as a succession of pulses which move from high order (low frequency) details to low order (high frequency) ones.
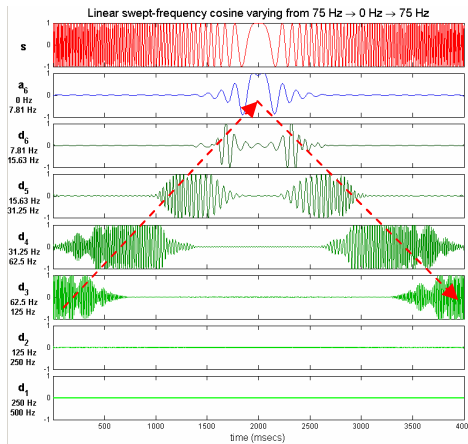
Fig. 7. Wavelet decomposition of a linear swept-frequency cosine.

3. *Complex signal*

A complex signal, analogous to the one present in machines with mixed eccentricity during a startup, has been generated by modulating the amplitude of a 45 Hz cosine with another linear swept-frequency cosine signal, with a frequency growing proportionally with time from 0 to 30 Hz. The DWT decomposition shown in Fig. 8 illustrates the effects of such modulation: the two sidebands characteristic of the modulation are first contained within the same level than the carrier (d_4), but as their frequencies change, they progressively move to the adjacent levels (d_5 for the 45-30=15 Hz lower sideband and d_3 for the 45+30=75 Hz upper sideband). At the end of the measurement time, single pure-tones appear within d_4 (carrier component), as well as d3 and d5 (sideband components) .
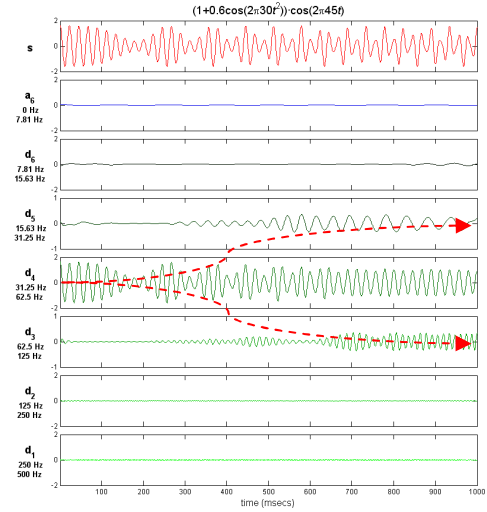
Fig.8. DWT decomposition of a complex signal.

IV. GUIDELINES FOR THE EASY APPLICATION OF THE METHODOLOGY

Fig.9 shows a scheme with the steps which should be followed in order to apply the DWT-based methodology for the diagnosis of electromechanical faults. Each step is detailed next.
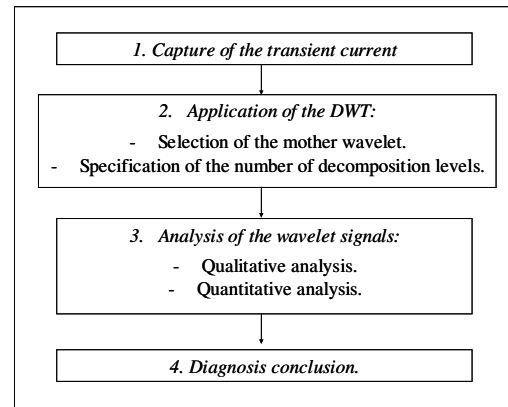
Fig. 9. Flowchart for the DWT-based diagnosis methodology.

A. *Capture of the transient current.*

The first step to be carried out consists of the capture of the transient current to be used as a basis for the diagnosis. One of the advantages of the methodology is its non-invasive nature, since the measurement of the current does not require interference with the normal operation of the machine. In addition, this is a quantity easy to be measured with very simple equipment as, for instance, the usually already existing current transformer mounted on the motor supply circuit, a shunt and a digital oscilloscope.

It must be considered, when capturing the transient signal, that the sampling frequency f_s plays an important role. Taking into account the Nyquist criterion, a very high sampling frequency is not mandatory for the application of the method [31], since the most important fault components are usually in the low-frequency region. Sampling frequencies of 2 or 5 ksamples/s (standard in data acquisition devices) enable good resolution analyses and, according to (6) and (7), provide two

different sets of frequency bands limits. However, a higher sampling frequency (for instance, 20 ksamples/s) enables to obtain -by decimation of sampled signal- new auxiliar sampling rates f'_s providing additional flexibility in the selection of the limits of the bands.

A practical remark is that, due to the non-ideal filtering carried out by the wavelet signals (Fig. 3), it is advisable not to set the limits of the band of the wavelet signal containing the fundamental frequency f, very close to this frequency. Otherwise, this component could be partially filtered within the adjacent bands masking the evolution of other components within these bands, due to its much higher amplitude. Typically, sampling frequencies being dyadic multiples of around 40 Hz (for instance, 5000 samp./s) are recommended for the application of the method.

B. Application of the DWT

In this work, MATLAB Wavelet Toolbox is used, although other software packages could be perfectly suitable for applying the methodology. Prior application of the DWT, the type of wavelet mother and the number of decomposition levels must be selected.

B.1. Selection of the mother wavelet.

An important step is the selection of the mother wavelet to carry out the analysis. The selected mother wavelet is related to the coefficients of the filters used in the filtering process inherent to the DWT [40, 41]. During these last decades, several wavelet families with rather different mathematical properties have been developed; infinite supported wavelets (Gaussian, Mexican Hat, Morlet, Meyer…) and wavelets with compact support (orthogonal wavelets, such as Daubechies or Coiflet, and biorthogonal wavelets) have been proposed. In some fields of the science, some families have shown better results for particular applications.

Nevertheless, regarding the transient extraction of the fault components, the experience achieved after the development of multiple tests shows that a wide variety of wavelet families can lead to satisfactory results.

However it has to be remarked that, in the case of compactly supported wavelets, once the wavelet family is selected, it is advisable to carry out the DWT using a high-order mother wavelet, this is, a wavelet with an associated filter with a large number of coefficients. If a low-order wavelet is used, the frequency response gets worse and the overlap between adjacent frequency bands, shown in Fig. 3, increases. Daubechies or Symlet with orders higher than 20 and 10, respectively, have shown satisfactory results. Also dmeyer, within the infinite support wavelets, has behaved very well.

In this paper, Daubechies-44 and dmeyer have been the mother wavelets used for the DWT analyses.

B.2. Specification of the number of decomposition levels.

The number of decomposition levels is determined by the low frequency components to be traced. The lower the frequency components to be extracted, the higher the number of decomposition levels of the DWT. So, the evolution of these components will be reflected through the high-level signals resulting from the analysis.

Typically, for the extraction of the frequency components caused by rotor asymmetries or even eccentricities, the number of decomposition levels should be equal or higher than that of the detail signal containing the fundamental frequency. This number of decomposition levels (n_f) is given by (8) [32]:

$$n_f = \text{integer}\left[\frac{\log(f_s / f)}{\log(2)}\right] \qquad (8)$$

For instance, considering f_s=5000 samples/s and f= 50Hz, the application of (8) leads to $n_f = 6$; for f_s=2000 samples/s, $n_f = 5$.

According to (6) and (7), the frequency bands associated with each wavelet signal are the ones shown in Table I.

Table I. Frequency bands for the wavelet signals

Level	Frequency band f_s=5000samp/s	Frequency band f_s=2000samp/s
d1	1250 – 2500 Hz	500 – 1000 Hz
d2	625 – 1250 Hz	250 – 500 Hz
d3	312.5 – 625 Hz	125 – 250 Hz
d4	156.25 – 312.5 Hz	62.5 – 125 Hz
d5	78.12 – 156.25 Hz	31.25 – 62.5 Hz
d6	39.06 – 78.12 Hz	15.625 – 31.25 Hz
a6	0 – 39.06 Hz	0 – 15.625 Hz

Once the mother wavelet and the number of decomposition levels have been selected, it is possible to carry out the DWT of the analysed signal, obtaining wavelet decomposition graphics as those shown in Figs. 10 to 16.

C. Analysis of the wavelet signals.

The next step to be carried out consists of the study of the wavelet signals resulting from the DWT. Two different and complementary types of analyses should be carried out: a qualitative analysis and a quantitative analysis.

C.1. Qualitative analysis

The aim of the qualitative analysis is to detect the presence of characteristic patterns caused by the evolution of the slip-dependant fault components during the transient, through the oscillations appearing in the wavelet signals. In the next section detailed analyses will be done for some cases including different types of faults and operation conditions.

C.2. Quantitative analysis

Once the condition of the machine has been preliminarily diagnosed, using the qualitative identification of characteristic patterns, it is advisable to compute quantification parameters defined for the corresponding fault, in order to assess the degree of failure in the machine. These parameters can also be used for generating alert signals in non-supervised monitorized systems; although alerts based on quantitative parameters are no as reliable as the identification of a characteristic pattern, they have the advantage of being much easier to be implemented.

In the last section some non-dimentional parameters will be introduced and computed for the cases qualitatively analyzed in the Section V.

D. Diagnosis conclusion.

Once the qualitative patterns associated with a particular fault have been detected and the failure severity has been quantified, the diagnosis conclusion can be reached.

An automation of the diagnostic process can be achieved with modern artificial intelligence techniques, such as neural networks, fuzzy logic or genetic algorithms. These could recognize automatically the patterns and compute the quantification indicators, providing a conclusion regarding the condition of the machine.

V. COMPILATION OF DIAGNOSTIC CASES

In this section the proposed methodology is applied for diagnosing several machines under different fault and operation conditions. A detailed interpretation of the signals resulting from the DWT is provided for each case.

The tests were performed in the laboratory, using commercial cage motors with 4 poles, 28 rotor bars, rated 1.1 kW, 400V, 50 Hz. A phase current was used as diagnostic signal; this current was captured using a 15/5, class 0.5 current transformer and a 1A, 60 mV shunt; the resulting voltage signal was captured by means a digital oscilloscope with a sampling frequency f_s = 5000 samples/s, and finally transferred to a PC for the analyses. The standard MATLAB Wavelet Toolbox was used for performing the DWT of the signals; Daubechies-44 was selected as mother wavelet.

A. Diagnosis of a healthy machine through the startup current

In this test, the induction motor was started direct on line, driving a high inertia load leading to a starting time of 6 s.

Fig. 10 shows the sampled startup current (signal s, at the top) and the signals resulting from the DWT with n=6 (*a6…d1*). These graphs can be explained as follows:

The detail *d6* practically reproduces the analyzed startup current. This is because, for the sampling frequency used the frequency band corresponding to this signal is [39.06, 78.12] Hz (see Table I), and so, includes the fundamental component of the current, which is more than 30 times greater than the rest of components.

- The approximation a6 does not show any relevant pattern, once the initial oscillations due to electromagnetic transient and border effects are extinguished. This means that there are no significant low frequency components (below 39,06 Hz) within the signal.

- Regarding the details *d5, d4, d3* a clear pattern can be observed. According to Section III, this pattern is produced by a component with frequency increasing with time; at the beginning of the startup, this component is included within the detail d6; consequently it is masked by the fundamental component. At t≈1.3 s, its frequency becomes higher than 78.012 Hz and the component penetrates within the detail d5. As time (or rotor speed) increases, the frequency does, moving to *d4* at t≈2.2 s, crossing successively the frequency bands of *d4* ([156.25 – 312.5 Hz]), and d3 ([312.5 – 625 Hz]), and
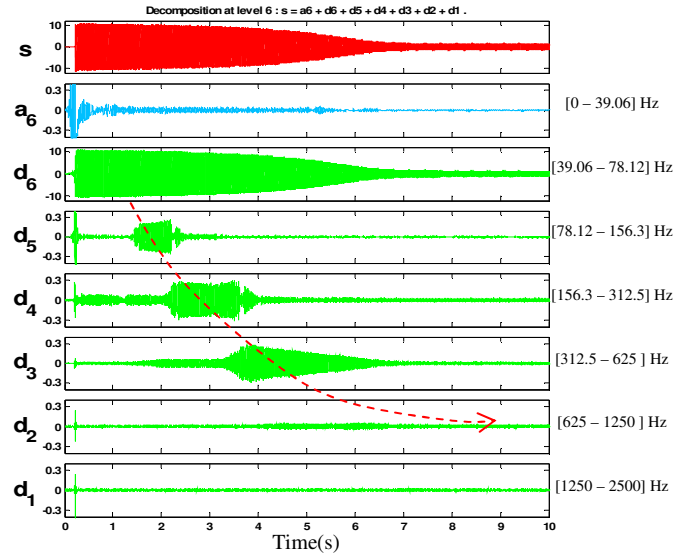

Fig. 10. DWT of the startup current of a healthy machine

finally remaining within *d2* when the steady-state is reached.

The pattern above described fits well the evolution during the startup of the Principal Slot Harmonic (I_{PSH}) of the machine, the frequency of which, a function of slip [43], is given by:

$$f_{PSH} = [14 \cdot (1-s) - 1] \cdot f \qquad (9)$$

At the beginning of startup s≈1 and f_{PSH}≈50Hz. As slip decreases f_{PSH} increases, reaching a constant value f_{PSH}≈650 Hz in steady state (s≈0). Fourier analysis of the stationary portion of *d2* confirms the previous interpretation, showing a predominant component of 640 Hz .

So, this pattern, which can be almost always found in the DWT of induction motors startup current, is not caused by the presence of any fault.

-The detail *d1* includes the high frequency components of the signal with frequencies in the interval ([1250 – 2500 Hz]); nothing relevant is observed in this detail signal.

B. Diagnosis of a machine with one broken bar through the startup current.

The previous test was repeated, but using a machine in which a rotor bar was artificially broken by drilling a hole at the junction point between the bar and the short-circuit ring. Fig.11 shows the DWT of the startup current for this case. Comparison between Figs.10 and 11 shows that the bar breakage is clearly detected through the alteration of the approximation a6 (or in general, the approximation of the same level as that of the detail containing the fundamental component); the change in this signal, as justified in [32], is caused by the left sideband component; its amplitude increases substantially when a rotor asymmetry is present and its frequency evolves during almost the whole startup within the frequency band of a6; it should be highlighted the similitude between the waveform of the approximation a6 and the theoretical evolution of the left sideband component during the startup, shown in Fig.1. This fact makes the diagnosis
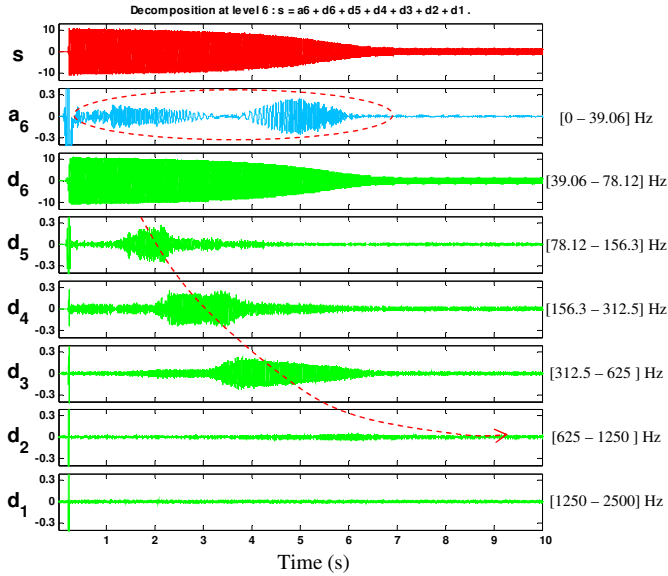
Fig. 11. DWT of the startup current of a machine with a broken bar. Diagnostic based on left sideband extraction

based on the approximation signal very reliable, since it is very unlikely that the pattern in a6 could be caused by a fault or perturbation different from a rotor asymmetry.

An alternative way for detecting a rotor asymmetry is shown in Fig.12; in this approach the number of DWT decomposition levels is increased up to 9 (3 more than the level of the detail signal containing the fundamental component). In this way the evolution of the sideband along the startup is spread across four consecutive wavelet signals (d7, d8, d9, a9), with frequency bands covering from near the main frequency to zero Hz. A clear pattern can be observed in these signals which, according to the precedents sections, corresponds to a component with decreasing frequency in the time interval 1<t<3 s and then, increasing frequency between t=3 and t=6. This also constitutes a reliable signature for the left sideband identification.
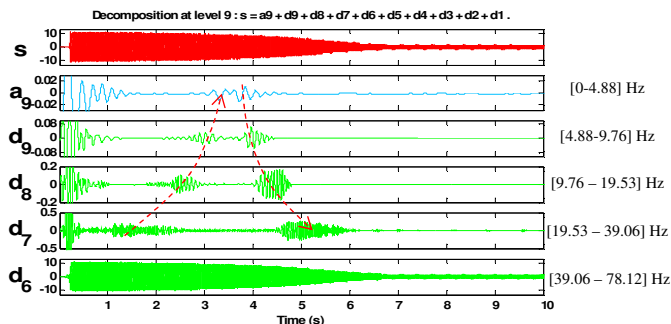

Fig12. DWT of the startup current of a machine with a broken bar. Diagnostic based on the characteristic pattern of low frequency wavelets signals.

C. Diagnosis of a machine with one broken bar through the plugging current

Figs. 13 and 14 show the DWT of stator current during a plugging transient. Both figures exhibit the characteristic pattern of a component with decreasing frequency, which successively crosses through the bands of d2, d3, d4, d5 and

finally, it disappears masked by the fundamental component when it goes within d6. This pattern is caused by the principal slot harmonic, which according to (9), when the main field reverses has a frequency slightly lower than 650 Hz; its frequency decreases as the slip decreases and finally it becomes equal to main frequency when the rotor stops (*s*=1) ; this pattern is not related with the fault and so, it is not useful for diagnosis purposes.

On the other hand, there is a noticeable difference between the details d5 in the cases of healthy and faulty machine. For the faulty machine (Fig.14), the left sideband component is clearly observable in the first half of the signal. There, it can be seen the characteristic decreasing frequency and a general waveform fitting that of the left sideband deduced theoretically (see Fig.2). From t ≈1.2 s. the sideband disappears, because its frequency gets below the lower limit of the frequency band corresponding to d5 and so, penetrates within d6, where it is masked by the fundamental component.
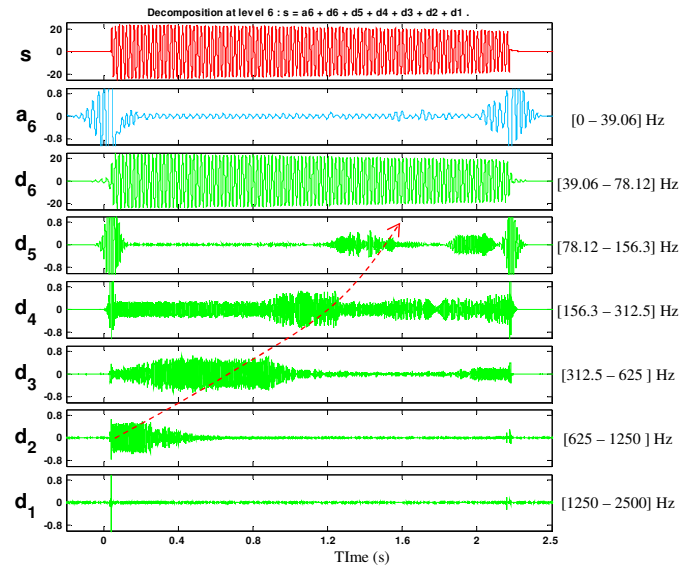

Fig. 13. DWT of the plugging current of a healthy machine

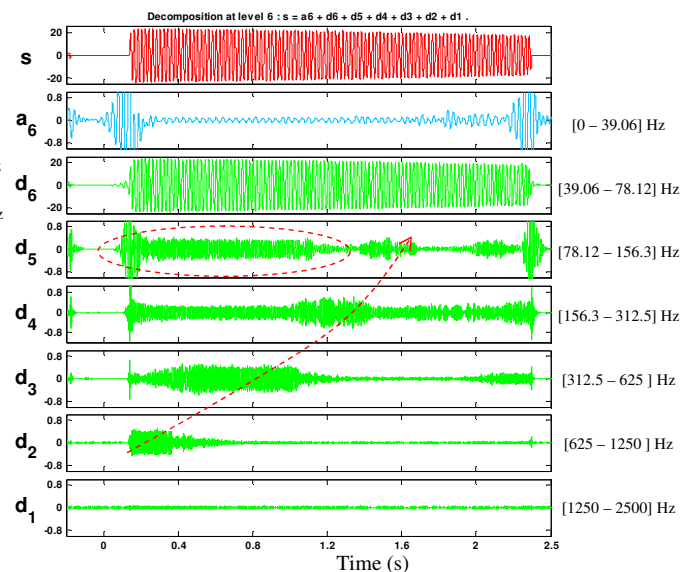
Fig. 14. DWT of the plugging current of a machine wit a broken bar

Therefore, the observation of that detail (the one with the next level lower than that containing the fundamental component), is a suitable method for confirming a rotor asymmetry, in machines stopped through plug braking.

D. Diagnosis of a machine with mixed eccentricity through the startup current

Before carrying out this test, it was necessary to prepare a motor introducing a certain degree of eccentricity in it. This was achieved by sanding down the inner and outer rings of the bearings, so that a slight play was achieved between the bearing and the shaft (for dynamic eccentricity) and between the bearing and its housing (for static eccentricity). Conventional Fourier analysis shows steady-state mixed eccentricity related components $(f \pm f_r)$, increased by a factor of three after this process growing their amplitude from 0.5% of the fundamental amplitude to 1.6%.

Figs.15 and 16 show respectively the DWT of the startup current before and after modifying the bearings; only the significant wavelet signals for this diagnosis are shown, this is, the signals containing the related eccentricity components $(f \pm f_r)$ during the startup. Comparing both figures, clear changes in the waveforms of d4 and a5 can be observed. Fig.16 (faulty machine) shows a pattern similar to that displayed in Fig.8; this pattern is produced by the components $(f \pm f_r)$ that are included within the detail d5 at the beginning of startup; as the rotor speed increases their frequencies change, reaching the limits of the band of d5 when the startup is almost finished. From this point, the decreasing component $(f - f_r)$ moves into a5 and the increasing component $(f + f_r)$ moves into d4. Subsequently, the diagnosis based on the DWT not only detects the fault through the increase of the amplitudes of the signals, like the steady-state based analyses, but also through the characteristic pattern due to the progressive increment in this amplitudes during the transient. This fact enables a more reliable diagnosis of the fault.

An interesting practical remark should be done; for this test, the sampling frequency f_s =5000 samp./s was not suitable, since it leads to an upper limit of the frequency band of the detail containing the fundamental component (d5) approximately equal to 80 Hz, above the frequency of the $(f + f_r)$ component at steady state. On the other hand, a sampling frequency f_s =2000 samp./s sets the upper limit of that band at 60 Hz, too near of fundamental frequency, which pollutes the detail d4. So, a sampling frequency f_s =20000 samp./s was finally used; the sampled signal was then decimated by 9, leading to a new sampling frequency f'_s =2222,2 samp./s, which leads to the bands limits of Figs.15 and 16. With these limits, the fundamental component is centred within the frequency band of d5, and it does not pollute at all neither d4 nor a5; this enables the clear observation of the eccentricity pattern.
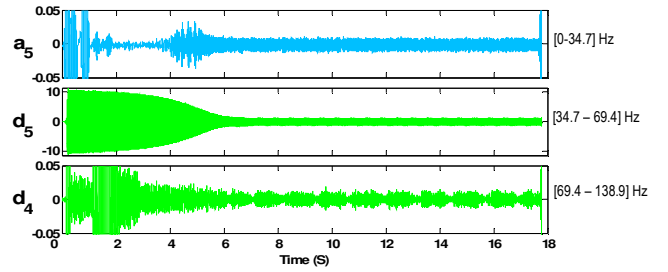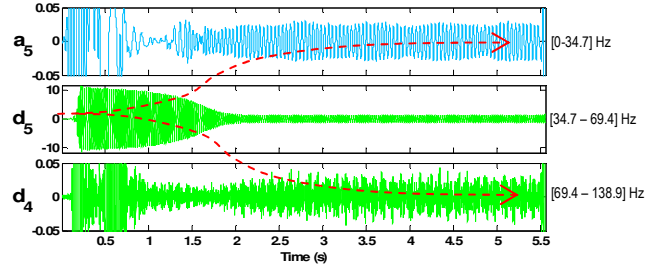

Fig. 15. DWT of the startup current;Healthy machine

Fig. 16. DWT of the startup current: Machine with eccentricity

VI. DEFINITION OF NON-DIMENSIONAL QUANTIFICATION PARAMETERS

The previous qualitative analyses show that all the faulty conditions analyzed imply that oscillations reflecting the evolution of the fault components appear in one or several wavelet signals. These oscillations lead to increases in the energy of the involved wavelet signals, which can be used as a basis for defining the parameters for the quantification of the severity of the fault.

In (10) a general expression is given for calculating non-dimensional parameters based on the increment of the energy of a wavelet signal:

$$\gamma_{w_n}(dB) = 10 \cdot \log \left[\frac{\sum_{j=Nb}^{Ns} i_j^2}{\sum_{j=Nb}^{Ns} [w_n(j)]^2} \right] \qquad (10)$$

where i_j is the value of the jth sample of the current signal; $w_n(j)$ is the j element of the wavelet signal affected by the fault (detail or approximation of nth order); N_s is the number of samples of the signal, until the fault-related oscillations disappear in the wavelet signal and N_b is the number of samples between the origin of the signals and the beginning of the oscillations. The parameters calculated by (10) represent the ratio between the energy of the startup current signal and the energy of the wavelet signal used for the quantification, within the referred time interval, expressed in dB. Table II compares the value of such parameters for healthy and faulty machines, in the cases analyzed in the previous section; the proposed parameters suffer significant reductions, above 10 dB in all the cases, when the fault occurs.

Table II. Calculated quantification parameters

Test	Wavelt signal, w_n	N_b	N_s	Healthy machine $\gamma_{wn\,(dB)}$	Faulty machine $\gamma_{wn(dB)}$
Startup(Fig.12-13)	a6	5000	30000	49.58	38.19 (1 broken bar)
Startup(Fig.12-14)	d7	5000	30000	49.64	39.19 (1 broken bar)
Plugging(Fig.15-16)	d5	9500	14000	38,23	19.47(1 broken bar)

VII. CONCLUSIONS

This paper presents a methodology for the diagnosis of rotor asymmetries and mixed eccentricities in cage induction motors through the application of the DWT. It is proved that rotor asymmetries and mixed eccentricities can be diagnosed through the characteristics patterns caused by their associated faults components in the DWT of stator current, during transients involving speed variations. The patterns caused by rotor asymmetries in the DWT of startup and plugging stator currents as well as that caused by mixed eccentricities in the DWT of startup current are described and verified by laboratory tests of commercial induction motors. Physical interpretations of these patterns based on electrical machine theory and DWT properties are also given. The understanding of the origin of these patterns enables the definition of non-dimensional parameters for fault severity quantification, which have proven to be very sensible, according to the results of the tests.

The proposed methodology can be considered as extension of traditional MCSA methods to transient regimes, in which the diagnosis of the fault is based not only on the harmonics existing in the current signal, but also on their characteristic evolution with time.

ACKNOWLEDGMENTS

REFERENCES

[1] M. H. Benbouzid, "A review of induction motors signature analysis as a medium for faults detection" *IEEE Transactions on Industrial Electronics*, Vol. 47, No. 5, October 2000.

[2] F. Filippetti, G. Franceschini, C. Tassoni, P. Vas, "Recent developments of induction motor drives fault diagnosis using AI techniques", *IEEE Transactions on Industrial Electronics*, Vol. 47, No. 5, October 2000, pp 994-1004.

[3] A. Bellini, F. Filippetti, G. Franceschini, C. Tassoni, G.B. Kliman, "Quantitative Evaluation of Induction Motor Broken Bars by Means of Electrical Signature Analysis", *IEEE Transactions on Industry Applications*, Vol. 37, No. 5, September/October 2001, pp 1248-1255.

[4] J.R Cameron et W.T. Thomson and A.B. Dow, "Vibration and current monitoring for detecting airgap eccentricity in large induction motors," *IEE Proceedings,* vol. 133, pt. B, no. 3, May 1986, pp. 155-163.

[5] G.M. Joksimovic and J. Penman, " The Detection of Inter-Turn Short Circuits in the Stator Winding of Operating Motors," *IEEE Transactions on Industrial Electronics*, Vol. 47, No. 5, October 2000, pp. 1078-1084.

[6] A. Stavrou, H.G. Sedding and J. Penman, " Current Monitoring for Detecting Inter-turn Short-circuits in Induction Motors," *IEEE Transactions on Energy Conversion*, Vol. 16, No. 1, March 2001, pp. 32-37.

[7] R.R. Schoen and T.G. Habetler. "Evaluation and Implementation of a System to Eliminate Arbitrary Load Effects in Current-Based Monitoring of Induction Machines," *IEEE Transactions on Industry Applications*, Vol. 33, No. 6, November/December 1997, pp. 1571-1577.

[8] J. Antonino-Daviu, M. Riera-Guasp, J. Roger-Folch and M.P. Molina, "Validation of a New Method for the Diagnosis of Rotor bar Failures via Wavelet Transformation in Industrial Induction Machines," *IEEE Transactions on Industry Applications*, Vol. 42, No. 4, July/August 2006, pp. 990-996.

[9] J. Antonino-Daviu, P. Jover, M. Riera-Guasp, J. Roger-Folch and A. Arkkio, "DWT Analysis of Numerical and Experimental Data for the Diagnosis of Dynamic Eccentricities in Induction Motors", *Mechanical Systems and Signal Processing*, *Elsevier*, Vol. 21, No. 6, August 2007, pp. 2575-2589.

[10] L. Kerzenbaum, C.F. Landy, "The existence of large inter-bar currents in three phase squirrel cage motors with rotor bar and/or end-ring faults", *IEEE Transactions on Power Apparatus and Systems*, Vol. PAS-103, No. 7, July 1984, pp. 1854-1862.

[11] J.F. Watson, S. Elder, "Transient analysis of the line current as a fault detection technique for 3-phase induction motors," *Proc. of the International Conference on Electrical Machines, ICEM'92*, 15-17 September 1992, Manchester, pp. 1241-1245.

[12] W.T. Thomson, N.D. Deans, R.A. Leonard and A.J. Milne, "Monitoring strategy for discriminating between different types of rotor defects in induction motors," *Proc. Univ. Power Engineering Conference*, 1983, pp.241-246

[13] Q.Qiu Arui, "Diagnosis of rotor fault in squirrel cage induction motors using time-varying frequency spectrum of starting stator current," *Proc. Chinese Soc. Elect. Eng.*, vol. 15, July 1995, pp. 267-273

[14] S. Elder, J.F. Watson and W.T. Thomson, "Fault detection in induction motors as a result of transient analysis" *Proc. IEE 4th International Conference on Electrical Machines and Drives.* London. 13-15 September 1989, pp 182-186.

[15] R. Burnett, J.F. Watson and S. Elder, "The application of modern signal processing techniques to rotor fault detection and location within three phase induction motors," *European Signal Processing Journal*, Vol. 49, pp. 426-431, 1996

[16] J.F. Watson, "The use of line current as a condition monitoring tool for three phase induction motors" *IEE Colloquium on Design, Operation ands Maintenance of High Voltage* (3.3 kV to 11 kV) Electric Motors for process Plant. April 1999. pp. 7/1-7/4

[17] J.F. Watson, N.C. Paterson, "Improved techniques for rotor fault detection in three-phase induction motors", *The 1998 IEEE Industry Applications Conference, 1998. Thirty-Third IAS Annual Meeting.*, vol.1, pp 271-277, 12-15 Oct 1998.

[18] H. Douglas, P. Pillay, and A. Ziarani , "Broken rotor bar detection in induction machines with transient operating speeds," *IEEE Transactions on Energy Conversion*, vol. 20, no. 1, pp. 135-141, March 2005.

[19] Z. Zhang and Z. Ren, "A novel detection method of motor broken rotor bars based on wavelet ridge," *IEEE Transactions on Energy Conversion*, vol. 18, no. 3, pp. 417-423, September 2003.

[20] W.G. Zanardelli, E.G. Strangas, H.K. Khalil, J.M. Miller "Wavelet-based methods for the prognosis of mechanical and electrical failures in electric motors", *Mechanical Systems and Signal Processing*. *Elsevier*. No. 19, 2005. pp. 411-426.

[21] S.H. Kia, H. Henao and G-A. Capolino, "Diagnosis of broken bar fault in induction machines using discrete wavelet transform without slip estimation," 42nd *IAS Annual Meeting,* New Orleans (USA), September 2007 (CD-ROM).

[22] F. Briz, M.W. Degnert, P. Garcia, D. Bragado, "Broken rotor bar detection in line-fed induction machines using complex wavelet analysis of startup transients," 42nd *IAS Annual Meeting*, New Orleans (USA), September 2007 (CD-ROM).

[23] S. Rajagopalan, J.M. Aller, J.A. Restrepo, T.G. Habetler and R.G. Harley, "Analytic-Wavelet-Ridge-Based Detection of Dynamic Eccentricity in Brushless Direct Current (BLDC) Motors Functioning Under Dynamic Operating Conditions", *IEEE Transactions on Industrial Electronics*, vol. 54, no. 3, pp. 1410-1419, June 2007.

[24] Z. Ye, B. Wu, A. Sadeghian, "Current signature analysis of induction motor mechanical faults by wavelet packet decomposition", *IEEE Transactions on Industrial Electronics*, Vol. 50, No. 6, 2003, pp.1217-1228.

[25] W. Rams, J. Rusek, "Practical Diagnosis of Induction Machines Operated in Power Plant Auxiliaries", 2005 *IEEE St. Petersburg PowerTech Proceedings*, St. Petersburg 27-30.06.2005.

[26] J. Antonino-Daviu, J.Rusek, M. Riera-Guasp, J. Roger-Folch and V. Climente, "Case Histories in large motors: Diagnosis of electromechanical faults through the extraction of characteristic components during the startup", Proc. *6th IEEE International Symposium on Diagnostics, Electric Machines, Power Electronics and Drives SDEMPED 2007*, Krakow, Poland, September 2007.

[27] J. Antonino-Daviu, M. Riera-Guasp, J. Roger-Folch and R.B. Pérez, "An Analytical Comparison between DWT and Hilbert-Huang-Based Methods for the Diagnosis of Rotor Asymmetries in Induction Machines", *Conference Record of the 42nd IAS Annual Meeting*, New Orleans, USA, September 2007, pp. 1932-1939.

[28] V.K. Rai, A.R. Mohanty, "Bearing Fault Diagnosis using FFT of intrinsic mode functions in Hilbert-Huang transform," *Mechanical Systems and Signal Processing*, Elsevier, Vol. 21, No. 6, August 2007, pp. 2607-2615.

[29] Z.K. Peng, P.W. Tse, F.L. Chu, "A Comparison Study of Improved Hilbert-Huang Transform and Wavelet Transform: Application to Fault Diagnosis for Rolling Bearing", *Mechanical Systems and Signal Processing*, Elsevier, Vol. 19, 2005, pp. 974-988.

[30] D. Yu, J. Cheng and Y. Yang, "Application of EMD method and Hilbert spectrum to the fault diagnosis of roller bearings", *Mechanical Systems and Signal Processing*, Elsevier, Vol. 19, 2005, pp. 258-270.

[31] J. Antonino-Daviu, M. Riera-Guasp, J. Roger-Folch, F. Martínez-Giménez, A. Peris, "Application and Optimization of the Discrete Wavelet Transform for the Detection of Broken Rotor Bars in Induction Machines". *Applied and Computational Harmonic Analysis*, Elsevier, Vol. 21, September 2006, pp. 268-279.

[32] M. Riera-Guasp, J. Antonino-Daviu, J. Roger-Folch and M.P. Molina, "The Use of the Wavelet Approximation Signal as a Tool for the Diagnosis and Quantification of Rotor Bar Failures," *IEEE Transactions on Industry Applications* (In press).

[33] M. Fernández Cabanas, M. García Melero, G. Alonso Orcajo, J.M. Cano Rodríguez, J. Solares Sariego. *Técnicas para el Mantenimiento y Diagnóstico de Máquinas Eléctricas Rotativas*. Ed. Marcombo.

[34] S.M.A. Cruz and A.J.M. Cardoso, "Diagnosis of Rotor Faults in Closed-Loop Induction Motor Drives", *Conference Record of the 41st IAS Annual Meeting*, Vol. 5, Tampa, USA, October 2006, pp. 2346-2353.

[35] W.Deleroi "Squirrel cage motor with broken bar in the rotor – physical phenomena and their experimental assessment", *Proc. ICEM'82*. Budapest, Hungary, 1982, pp. 767-770

[36] J.Stepina "Fundamental equations of the space vector analysis of electrical machines". *Acta technica ČSAV*, Nº2, 1968, pp.184-198

[37] M.G. Say, *"Alternating current machines"*. Ed. Pitman books Ltd., London, 1982

[38] S. Nandi, H.A. Toliyat, "Condition monitoring and fault diagnosis of electrical motors- A review", *IEEE Transactions on Energy Conversion*, Vol. 20, No. 4, December 2005, pp.719-729.

[39] D. G. Dorrell, W. T. Thomson, and S. Roach, "Analysis of airgap flux, current, vibration signals as a function of the combination of static and dynamic airgap eccentricity in 3-phase induction motors," *IEEE Trans. Ind. Appl.*, Vol. 33, No. 1, pp. 24–34, Jan./Feb. 1997.

[40] C.S. Burrus, R.A. Gopinath and H. Guo, *Introduction to Wavelets and Wavelet Transforms. A primer*, Prentice Hall, 1998.

[41] R.Polikar, 'The wavelet tutorial' *http://engineering.rowan.edu/~polikar/WAVELETS/WTtutorial.html*

[42] T. Tarasiuk, "Hybrid wavelet-Fourier Spectrum Analysis," *IEEE Transactions on Power Delivery*, vol. 19, no. 3, pp. 957-964, July 2004.

[43] Nandi, S.; Ahmed, S.; Toliyat, H.;" Detection of Rotor Slot and Other Eccentricity-Related Harmonics in a Three-Phase Induction Motor with Different Rotor Cages" *Power Engineering Review, IEEE Volume 21, Issue 9, Sept. 2001 Page(s):62 – 62*.